BAC-MP4 Predictions of Thermochemistry for Gas-Phase Antimony Compounds in the Sb−H−C−O−Cl System

Andrew J. Skulan,[†] Ida M. B. Nielsen,[†] Carl F. Melius,[‡] and Mark D. Allendorf*,[†]

Sandia National Laboratories, Livermore, California 94551-0969, and Lawrence Livermore National Laboratory, Livermore, California 94550

Received: December 22, 2005; In Final Form: February 24, 2006

Calibrated by both experimental data and high-level coupled-cluster calculations, the BAC-MP4 methodology was applied to 51 SbL$_n$ (L = H, CH$_3$, C$_2$H$_5$, Cl, and OH, n = 1−5) molecules, providing calculated heats of formation and associated thermodynamic parameters. These data identify a linear variation in heats of formation with ligand substitution, trends in bond dissociation energies (BDEs) with ligand identity [BDE(Sb−C$_2$H$_5$) < BDE(Sb−CH$_3$) < BDE(Sb−H) < BDE(Sb−Cl) < BDE(Sb−OH)], and a monotonic decrease in BDE upon successive ligand elimination. The linear variation in BDE is consistent with the behavior of other group V elements, in contrast to the characteristic high−low−high trend of adjacent group III (In) and group IV (Sn) elements. Additionally, these data complement those of previous studies of metal−organic species and provide a foundation of thermochemical data that can aid in the selection of CVD precursors and deposition conditions for the growth of antimony-containing materials.

I. Introduction

Groups III−V thin film materials are of considerable interest because they are semiconductors suited to a wide range of micro- and optoelectronics applications.[1−5] Antimony-containing materials, such as InSb, GaSb, and GaInAsSb, exhibit the smallest band gap of this class of semiconductors, making them good infrared detectors.[6,7] The synthesis of suitable antimony precursors has been of particular interest, as candidates such as SbH$_3$ decompose at room temperature, whereas Sb(CH$_3$)$_2$(H) is unstable above −78 °C.[1] Precursors successfully used in M−Sb (M = Al, Ga, In) films include Sb(CH$_3$)$_3$, Sb(C$_2$H$_5$)$_3$, Sb(CH$_3$)$_2$(*t*-C$_4$H$_9$), and Sb[(CH$_3$)$_2$N]$_3$.[5,8−13] Longer hydrocarbons are of interest because the Sb−C bond strength decreases with increasing ligand size,[1] but they are practically limited by the concurrent decrease in the volatility of the precursor.

In addition to the results of deposition experiments, a number of pyrolysis studies on metal−organic antimony compounds have been reported. Many of these were performed by String-fellow and co-workers and involved pyrolysis in a flow tube with mass spectrometric detection of reaction products.[14−16] These found that the major decomposition pathway for Sb(CH$_3$)$_3$,[15] Sb(C$_2$H$_5$)$_3$, and Sb(CH$_3$)$_2$(*i*-C$_3$H$_7$)[14] is radical elimination via homolytic cleavage of the Sb−C bond. In contrast, Sb(H)(*i*-C$_3$H$_7$)$_2$ is believed to proceed via a reductive elimination reaction generating Sb(*i*-C$_3$H$_7$) and propane.[16] An additional study with EPR detection of radical species expanded these results for Sb(CH$_3$)$_3$ and Sb(C$_2$H$_5$)$_3$, proposing that the initial ligand eliminated is a radical, L·, that is terminated by abstracting a proton from other SbL$_3$ molecules.[17]

When modeling the species present within a chemical vapor deposition (CVD) reactor, the thermochemical quantities of greatest interest are the molecular heats of formation, which permit calculation of reaction enthalpies and bond dissociation energies (BDEs). For processes such as pyrolysis where the number of molecules present changes during the reaction, entropic contributions to reaction spontaneity become important, necessitating consideration of reaction free energy and its variation with temperature. As with many metal−organic molecular systems,[18,19] a limited amount of experimental thermochemical data is available. Apart from the pyrolysis data described above, the National Bureau of Standards (NBS) tables[20] give the heats of formation of SbH$_3$, SbCl, SbCl$_2$, and SbCl$_3$. Additional reports have been made for the heats of formation of Sb(CH$_3$)$_3$[21−23] and Sb(C$_2$H$_5$)$_3$.[21,24] This short list is clearly inadequate for selecting metal−organic precursors for CVD applications and lacks the systematic approach required to evaluate a broader class of compounds, further reinforcing the need for the current study.

The BAC-MP4 approach applies a semiempirical bondwise correction to molecular enthalpies calculated at the MP4 level of theory. This has been found to deliver accurate thermochemical data for hydrocarbons and a wide range of main-group halides, hydroxides, and alkylated compounds.[25−28] Parallel studies on indium[18] and tin[19] compounds have verified that this method is applicable to period IV molecules.

This study presents the BAC-MP4 thermochemistry of a family of antimony compounds and the trends within these properties with ligand variation. The 51 compounds range from one- to five-coordinate and contain H, CH$_3$, C$_2$H$_5$, Cl, and OH ligands. These include SbX$_n$ (n = 1−3) and SbXY$_n$ (n = 1, 2) compounds, the ligand decomposition molecules Sb(H$_2$)O and Sb(H$_2$)CH$_2$, and the five-coordinate compounds Sb(Cl)$_5$ and Sb(Cl)$_3$(H)$_2$ and their elimination products. Their molecular geometries, heats of formation, entropies, and free energies of formation are tabulated in the text, and additional computational results, including geometric and vibrational data, and polynomial fits of thermodynamic data suitable for the CHEMKIN suite of reacting-flow codes[29] are included in the Supporting Information. These data are also available within the Thermodynamics Resource, a Web site that we developed to make high-

* Corresponding author. E-mail: mdallen@sandia.gov.
† Sandia National Laboratories.
‡ Lawrence Livermore National Laboratory.

temperature, computationally derived thermochemical data for gas-phase species available in a searchable database.[30]

II. Theoretical Methods

II.1. Ab Initio Reference Calculations. The BAC method requires a reference heat of formation for each antimony–ligand bond type to calibrate the bondwise $\Delta H_f°$ correction. No suitable heats of formation for antimony compounds with hydroxide ligands were found in the literature, so the heat of formation was computed for $Sb(OH)_3$ using high-level ab initio methods. The heat of formation for $Sb(OH)_3$ was computed from two isogyric reactions: (1) $Sb(OH)_3 + 3H_2 \rightarrow SbH_3 + 3H_2O$ and (2) $Sb(OH)_3 + \frac{3}{2}Cl_2 + \frac{3}{2}H_2 \rightarrow SbCl_3 + 3H_2O$. Geometries were optimized using the B3LYP density functional method with the {cc-pVTZ-PP, cc-pVTZ} basis sets.[31,32] In the basis set notation {basis1, basis2} used here, basis1 is the basis set used for Sb, and basis2 is the set employed for other atoms. The cc-pVXZ-PP sets use a small-core pseudopotential.[33] Reaction energies were computed at the CCSD(T)/{cc-pVDZ-PP, cc-pVDZ} level, and a {cc-pVDZ-PP, cc-pVDZ}→{cc-pVTZ-PP, cc-pVTZ} correction, computed using second-order Møller–Plesset perturbation theory (MP2), was applied. A zero-point vibrational energy correction was computed at the B3LYP/{cc-pVTZ-PP, cc-pVTZ} level, yielding reaction enthalpies at 0 K. The heat of formation for $Sb(OH)_3$ at 0 K was then computed using literature values for the heats of formation for SbH_3, $SbCl_3$, and H_2O.[20,34] The heats of formation computed from reactions 1 and 2 are −145.52 and −152.04 kcal/mol, respectively. Judging from the faster convergence observed in the computed reaction energy with respect to improving the employed level of theory for reaction 2, we weight the result obtained from reaction 2 somewhat higher and arrive at a value of −150 ± 4 kcal/mol for $\Delta H_f[Sb(OH)_3, 0 K]$.

Additionally, the heat of formation was computed for $Sb(CH_3)(H)_2$, employing the isogyric reaction $Sb(H)_3 + CH_4 \rightarrow Sb(CH_3)(H)_2 + H_2$. Geometries and harmonic vibrational frequencies were computed as described above, and the reaction energy was computed at the CCSD(T) level using the {cc-pVTZ-PP, cc-pVTZ} basis sets. Using literature values for the heat of formation for SbH_3 and CH_4 at 298 K,[35,36] the calculated heat of formation was $\Delta H_f[Sb(CH_3)(H)_2, 0 K] = 27.2 ± 4$ kcal/mol.

II.2. BAC-MP4. The BAC-MP4 method applies an empirical bond additivity correction (BAC) to the molecular electronic energy calculated by fourth-order Møller–Plesset perturbation theory (MP4). This approach has been successfully applied to a range of main-group elements spanning multiple groups and rows of the periodic table, including H, B, C, N, O, Al, Si, P, Cl, Sn, and In. BAC-MP4, as originally developed, optimizes molecular geometries using the 6-31G(d) basis set in conjunction with restricted Hartree–Fock (RHF) theory for closed-shell molecules and unrestricted Hartree–Fock (UHF) for open-shell molecules while energetics are calculated using 6-31G(d,p).[37–39] Internally consistent thermochemical data require that correct trends in bond lengths and angles for classes of related molecules be predicted, a condition fulfilled by HF geometry optimizations.[40–43] The absence of imaginary (negative) frequencies verifies that the final geometry-optimized structure is at an energy minimum. The frequencies are divided by an empirical scaling factor of 1.12 to account for the systematic overestimation of the vibrational frequencies at this level of theory[44] and are used in subsequent calculation of thermodynamic values. Electronic energies; atomization enthalpies; and, by extension, heats of formation are computed using MP4(SDTQ)/6-31G(d,p)

TABLE 1: BAC Parameters for Each Bond (A_{ij}) and Atom (B_k) Type

	Sb−H	Sb−C	Sb−O	Sb−Cl	C−H	O−H
A_{ij}(MP4)	244.1	649.4	639.5	1718.7	38.6	72.5

	Sb	H	C	O	Cl
B_k(MP4)	0.30	0.00	0.31	0.23	0.42

calculations [fourth-order Møller–Plesset perturbation theory with single, double, triple, and quadruple substitutions using the 6-31G(d,p) basis set].

However, because the 6-31G basis set has not yet been expanded to include antimony, a different basis set must be chosen. Consistent with previous extensions of the BAC-MP4 method to the Sn−H−C−Cl system[19] and the In−H−C−O−Cl system,[18] antimony is described by the CRENBL-ECP basis set.[45,46] The 1s−4p electrons are described by an effective core potential, while the valence $4d^{10}5s^25p^3$ electrons are modeled with an uncontracted Gaussian basis set containing 3s, 3p, and 4d functions. All BAC-MP4 calculations in this study were performed using Gaussian 98.[47]

The constituent BAC equations are given below (eqs 1−5) for the $X_i−X_j$ bond in the molecule $X_k−X_i−X_j$ and depend on three parameters, α_{ij}, A_{ij}, and B_k; the length of the bond in question (R_{ij}); and adjacent bond effects

$$E_{BAC}(X_i−X_j) = f_{ij}g_{kij} \tag{1}$$

where

$$f_{ij} = A_{ij}\exp(-\alpha_{ij}R_{ij}) \tag{2}$$

$$g_{kij} = (1 - h_{ik}h_{ij}) \tag{3}$$

$$h_{ik} = B_k\exp[-\alpha_{ik}(R_{ik} - 1.4\text{ Å})] \tag{4}$$

$$A_{ij} = (\Delta H_{f,ref}° - \Delta H_{f,calc}°)/[n\exp(-\alpha_{ij}R_{ij})g_{kij}] \tag{5}$$

A_{ij} acts as a reference magnitude for the bond additivity correction [i.e., $E_{BAC}(X_i−X_j) \propto A_{ij}$ from eqs 1 and 2] and is defined as the bondwise normalized energy difference between the reference $\Delta H_f°$ value and the calculated $\Delta H_f°$ value (eq 5). n is the number of a particular metal–ligand bond type in the reference molecule (e.g., $n = 3$ for SbH_3 as there are three Sb−H bonds). α_{ij} is a parameter that depends on the $i−j$ bond type. α_{C-C} is 3.8 Å^{-1}, and α_{O-C} is 2.14 Å^{-1}, whereas for all other bond types, α_{ij} is set to 2.0.[19] B_k (eq 4) corrects for the effects of neighboring atoms on the $X_i−X_j$ bond (eq 3) and depends on the identity of atom k. A_{ij}, α_{ij}, and B_k are specific to the level of theory used for the calculated $\Delta H_f°$ value {e.g., A_{ij}(MP4), using SbH_3 as the reference compound for the Sb−H bond, is $[\Delta H_{f,ref}°(SbH_3) - \Delta H_{f,MP4}°(SbH_3)]/[3\exp(-\alpha_{ij}R_{ij})g_{kij}]$}. These parameters are calculated from a set of reference compounds representing each of the bond types present in the set of molecules under investigation. R_{ij} is the bond distance in angstroms. Additional corrections for UHF instability and nonzero ground-state spin are described elsewhere.[48]

Table 1 lists the parameters A_{ij} for each bond type and B_k for each atom type. The reference heats of formation used to calculate A_{ij} for each antimony–ligand bond correction were (kcal/mol): $\Delta H_f°[SbH_3, 0 K] = 34.625,$[20] $\Delta H_f°[Sb(CH_3)_3, 0 K] = 15.037,$[22] $\Delta H_f°[Sb(Cl)_3, 0 K] = -74.57,$[20] and $\Delta H_f°[Sb(OH)_3, 0 K] = -150.0$ (vide supra). Ligand $\Delta H_f°(0 K)$ values used for bond dissociation energy

BAC-MP4 Predictions of Sb−H−C−O−Cl Thermochemistry

J. Phys. Chem. A, Vol. 110, No. 17, 2006 **5921**

(BDE) calculations were (kcal/mol): H, 52.1; CH_3, 34.9; C_2H_5, 28.8; OH, 9.5; Cl, 29.0; Sb, 62.7.

The sum of the BACs for each metal−ligand bond, the MP4(SDTQ) electronic energy, and the unscaled zero-point energy were combined to calculate $\Delta H_f°(0\ K)$. This result was used, along with statistical mechanics and the harmonic oscillator approximation, calculated geometries, and vibrational frequencies, to calculate the temperature-dependent molecular entropies, heat capacities, enthalpies, and free energies. Unscaled frequencies were used for determining the zero-point energy and $\Delta H_f°(0\ K)$ value, and the scaled frequencies were used to calculate thermochemistry at higher temperatures in order to maintain consistency with earlier papers in this series.[18,19,26,27,49−51] The minor differences that would have resulted from using scaled rather than unscaled frequencies to calculate $\Delta H_f°(0\ K)$ were taken into account by the BAC corrections. A hindered rotor was substituted for the vibrational modes involving rotating groups in order to properly account for their contributions to the molecular heat capacity and entropy.[52] The interpolation formulas of Pitzer and Gwinn[53] were used, and the barrier to rotation was determined from the formula reported by Benson[54] for a torsional vibration (calibrated to the barrier reported for the internal rotor in ethane,[55] 2.9 kcal mol^{-1})

$$V_0 = I_{red}\left(\frac{\nu}{134n}\right)^2 \qquad (6)$$

V_0 is the barrier height in kcal mol^{-1}, I_{red} is the reduced moment of inertia in amu Bohr^2, ν is the frequency of the internal rotor in cm^{-1}, and n is the rotational symmetry number of the rotating group. A rotational symmetry number of 3 was assigned to CH_3 groups; all other rotating groups were assigned a value of 2.[56]

Uncertainties due to inadequacies of the theoretical methods in describing a given molecule were estimated using an ad hoc method developed previously (eq 7) that extrapolates lower-level calculations[48]

$$\text{error(BAC-MP4)} =$$
$$\{1.0\ \text{kcal mol}^{-1} + (\Delta H_{BAC-MP4} - \Delta H_{BAC-MP3})^2 +$$
$$(\Delta H_{BAC-MP4} - \Delta H_{BAC-MP4SDQ})^2 +$$
$$0.25[E_{BAC}(\text{spin}_{S2})\ \text{or}\ E_{BAC}(\text{spin}_{UHF-I})]^2\}^{1/2} \quad (7)$$

Additionally, there is uncertainty due to limitations of literature data from which the BAC corrections were derived. This error scales with the number of bonds in the molecule and can increase the uncertainty estimates by a few kcal/mol. It is important to note that the use of different reference values would offset the entire body of calculated heats of formation, resulting in the calculated BDEs and reaction enthalpies being affected to a smaller degree than the individual heats of formation. Propagating these two independent sources of error through eqs 1−5 and 7 leads to a net uncertainty of ±2−4 kcal/mol.

The bond dissociation energy (BDE) is the heat of reaction for the dissociative reaction AB → A + B yielding two uncharged reaction products. BDEs, derived from the BAC-MP4 results, are presented at 298 K. When a reaction product is monoatomic or an individual ligand (e.g., CH_3, OH), the experimental heat of formation was used to calculate the bond energy, whereas for antimony-containing polyatomic dissociation products (such as ^3SbCl in the reaction $^2SbCl_2 \rightarrow {}^3SbCl + {}^2Cl$ to identify the BDE of the Sb−Cl bond of $^2SbCl_2$), the BAC-MP4 value was used.

III. Results and Discussion

III.1. Bond Lengths and Geometry. Antimony compounds of the form SbL_3 (L = H, CH_3, C_2H_5, OH, and Cl) are trigonal-pyramidal in shape. This is in contrast to the trigonal-planar InL_3 complexes and is due to repulsion from a lone electron pair on the antimony atom in these SbL_3 compounds. Table 2 lists calculated antimony−ligand bond lengths and angles for each species, as well as the MP4(SDTQ) BACs corresponding to all bonds in the molecule. Additional geometric information, including molecular structures in the form of Cartesian coordinates, moments of inertia, vibrational frequencies, and data concerning hindered rotors, is available on the Internet[30] and in Supporting Information.

A small variation in the computed bond distances is found for each of the Sb−L bond types, with Sb−C and Sb−O varying by 1.5% from their mean values, whereas Sb−H and Sb−Cl both varied by 1.0% from their mean values, consistent with previous studies on similar tin[19] and indium[18] compounds. Bond angles range from 95° to 100°, much less than the 109.5° bond angles of a regular tetrahedron, as the presence of the lone electron pair compresses the angle between the three ligands. The variation is similar to that calculated for tin compounds (109.5° ± 4.5°), whereas a greater variation is predicted for three-coordinate indium compound bond angles (111−136°). The latter might be larger because of the planar geometry of the indium compounds; their three X−M−Y angles sum to 360°, whereas for the corresponding trigonal-pyramidal antimony compounds, the angles sum to 286° ± 6°, leaving less space to accommodate a greater range of X−M−Y angles. The bond lengths of the two-coordinate SbXY compounds considered in this study are comparable to those of three-coordinate compounds, and the X−Sb−Y bond angles range from 91° to 98°.

Geometric isomers of the five-coordinate molecules $Sb(Cl)_5$, $Sb(Cl)_4(H)$, and $Sb(Cl)_3(H)_2$ and their four-coordinate elimination products were also investigated.[57] The five-coordinate molecules belong to the D_{3h} [$Sb(Cl)_5$], C_{3v} [ax-$Sb(Cl)_4(H)$], C_{2v} [eq-$Sb(Cl)_4(H)$], D_{3h} [$trans$-ax-$Sb(Cl)_3(H)_2$], and C_{2v} [cis-eq-$Sb(Cl)_3(H)_2$] symmetry point groups. The axial Sb−L bond lengths overlap with those of corresponding trigonal-pyramidal three-coordinate molecules, whereas the equatorial bonds are shorter than those of three-coordinate molecules by 0.05 Å on average. The axial ligand bonds are longer than the equatorial bonds for the same element, but they vary significantly by molecule, with $r(Sb-Cl_{ax}) - r(Sb-Cl_{eq})$ differences ranging from 0.02 Å in ax-$Sb(Cl)_4(H)$ to 0.11 Å in cis-eq-$Sb(Cl)_3(H)_2$.

III.2. Thermochemical Data. The heats of formation (0 K) at various levels of theory are presented in Table 3. These values show a small variation in the BAC-MPx- [x = 2, 3, 4(SDQ), 4(SDTQ)] calculated heats of formation with increasing levels of theory, indicating that the method is appropriate for this group of molecules for the basis sets chosen. On average, the molecular heat of formation varies by 1 kcal/mol across the four perturbation levels.

The $\Delta H_f°(0\ K)$ values of $^3Sb(L)$ molecules (L = H, CH_3, C_2H_5, Cl, OH) are lower in energy than those of the corresponding $^1Sb(L)$ compounds. This leads to a triplet instability[58] in the $^1Sb(L)$ molecules and a significantly greater variation of $\Delta H_f°(0\ K)$ with MPx method (2.6 kcal/mol, on average). The two highest-energy electrons of Sb(L) occupy a degenerate pair of 5p orbitals, making the triplet state more stable than the spin-paired singlet. $^1Sb(L)$ was higher in energy than $^3Sb(L)$ by 20−23 kcal/mol for H, CH_3, C_2H_5, and Cl compounds, whereas ^1SbOH was higher in energy by 11.2 kcal/mol. For correspond-

TABLE 2: Sb−L Bond Lengths (Å), BACs (kcal/mol), and X−In−Y Angles (deg)^a

	Sb−H length	BAC corr	Sb−C length	BAC corr	Sb−Cl length	BAC corr	Sb−O length	BAC corr	∠1	∠2	∠3
^{1}SbH	1.712	7.96									
^{3}SbH	1.714	7.93									
Sb(H)$_2$	1.707	8.03							91.6		
Sb(H)$_3$	1.701	8.13							93.1	93.1	93.1
^{1}Sb(CH$_3$)			2.181	8.27							
^{3}Sb(CH$_3$)			2.196	8.04							
Sb(CH$_3$)$_2$			2.184	8.20					94.3		
Sb(CH$_3$)$_3$			2.174	8.33					95.7	95.7	95.7
Sb(H)(CH$_3$)	1.711	7.96	2.185	8.21					93.7		
Sb(H)$_2$(CH$_3$)	1.705	8.07	2.176	8.36					92.8	95.3	95.3
Sb(H)(CH$_3$)$_2$	1.709	8.00	2.175	8.35					94.9	94.9	96.2
^{1}Sb(C$_2$H$_5$)			2.197	7.93							
^{3}Sb(C$_2$H$_5$)			2.209	7.74							
Sb(C$_2$H$_5$)$_2$			2.197	7.89					96.7		
Sb(C$_2$H$_5$)$_3$			2.186	8.04					95.8	95.8	95.8
Sb(H)(C$_2$H$_5$)	1.712	7.95	2.196	7.95					93.5		
Sb(H)$_2$(C$_2$H$_5$)	1.706	8.05	2.187	8.09					92.9	95.1	95.3
	1.705	8.06									
Sb(H)(C$_2$H$_5$)$_2$	1.710	7.99	2.186	8.06					94.8	95.0	98.6
			2.187	8.05							
^{1}SbCl					2.371	15.00					
^{3}SbCl					2.386	14.55					
Sb(Cl)$_2$					2.367	15.05			98.0		
Sb(Cl)$_3$					2.353	15.42			97.3	97.3	97.3
Sb(H)(Cl)	1.706	8.05			2.385	14.58			93.3		
Sb(H)$_2$(Cl)	1.700	8.14			2.384	14.60			92.1	94.5	94.5
Sb(H)(Cl)$_2$	1.699	8.16			2.367	15.07			93.3	93.3	98.7
Sb(CH$_3$)(Cl)			2.171	8.42	2.397	14.17			94.1		
Sb(CH$_3$)$_2$(Cl)			2.162	8.53	2.403	13.95			95.5	95.0	95.0
Sb(CH$_3$)(Cl)$_2$			2.153	8.69	2.376	14.73			94.4	94.4	98.5
^{1}Sb(OH)							1.952	12.84			
^{3}Sb(OH)							1.952	12.29			
Sb(OH)$_2$							1.962	12.52	96.3		
Sb(OH)$_3$							1.948	12.78	95.0	95.0	95.0
Sb(H)(OH)	1.705	8.07					1.972	12.33	91.8		
Sb(H)$_2$(OH)	1.712	7.95					1.962	12.57	91.3	97.4	97.4
Sb(H)(OH)$_2$	1.724	7.77					1.953	12.75	94.8	94.8	99.8
Sb(CH$_3$)(OH)			2.164	8.53			1.977	12.14	90.9		
Sb(CH$_3$)$_2$(OH)			2.159	8.56			1.978	12.07	95.1	94.4	94.4
Sb(CH$_3$)(OH)$_2$			2.137	8.95			1.961	12.46	91.8	91.8	99.1
Sb(Cl)(OH)					2.391	14.33	1.946	12.92	96.6		
Sb(Cl)$_2$(OH)					2.369	14.92	1.922	13.50	96.1	96.9	96.9
Sb(Cl)(OH)$_2$					2.393	14.22	1.931	13.23	94.9	94.9	99.5
Sb(H)$_2$(CH$_2$)	1.706	8.05	2.135	9.08					92.2	95.6	95.6
Sb(H)$_2$(O)	1.703	8.10					1.984	12.04	93.0	95.8	95.8
ax-Sb(Cl)$_3$(H)	1.673	8.60			2.412	13.73			119.6	119.6	119.6
$trans$-ax-Sb(Cl)$_3$(H)$_2$	1.665	8.74			2.369	14.95			120.0 (eq)	90 (eq-ax)	180 (ax)
cis-eq-Sb(Cl)$_3$(H)$_2$	1.656	8.89			2.4167 (2ax)	13.59			116.9 (eq Cl−Sb−Cl)	89.2 (eq-ax Cl−Sb−H)	176.6 (ax)
					2.3033 (eq)	17.03					
ax-Sb(Cl)$_4$					2.414 (3eq)	13.62			119.1 (eq)	119.1 (eq)	95.6 (eq-ax)
					2.3189 (ax)	16.45					
eq-Sb(Cl)$_4$					2.3206 (2eq)	16.39			100.1 (eq)	98.3 (eq-ax)	153.8 (ax)
					2.4475 (2ax)	12.74					
ax-Sb(Cl)$_4$(H)	1.675	8.57			2.3366 (3eq)	15.86			120 (eq)	90 (eq-ax)	180 (ax)
					2.3572 (ax)	15.22					
eq-Sb(Cl)$_4$(H)	1.662	8.79			2.3065 (2eq)	16.84			117.3 (eq)	90.6 (eq-ax)	177.6 (ax)
					2.389 (2ax)	14.30					
Sb(Cl)$_5$					2.3632 (2ax)	14.98			120 (eq)	90 (eq-ax)	180 (ax)
					2.3117 (3eq)	16.58					

^{a} Angles are ordered according to molecule name, e.g., for Sb(H)$_2$(Cl), ∠1 = ∠(H)−Sb−(H) = 92.1°, ∠2 = ∠(H)−Sb−(Cl) = 94.5°, ∠3 = ∠(H)−Sb−(Cl) = 94.5°.

ing indium (InL) and tin (SnL$_2$) species, the singlet is more stable, as the two nonbonding valence electrons spin-pair while occupying the relatively low-lying 5s orbital (vide infra).

Table 4 compares the BAC-MP4-calculated $\Delta H_f°$(298 K) values to the small number of available literature values. This comparison illustrates the need for a broad range of thermochemical data to aid the understanding of antimony gas-phase chemistry. Three of the literature values, i.e., those for SbH$_3$, Sb(CH$_3$)$_3$, and SbCl$_3$, were used to calibrate the BAC-MP4 corrections and, thus, coincide with the calculated heats of formation. The heat of formation reported for In(CH$_3$)$_3$ differs significantly from that obtained from a wide range of quantum chemical methods, including CCSD(T) calculations,[18,59,60] leading to concern that a similar discrepancy might exist for methyl-

TABLE 3: ΔH_f(0 K) at a Range of Levels of Theory: MP4, BAC-MP2, BAC-MP3, BAC-MP4(SDQ), BAC-MP4(SDTQ)^a

	MP4	spin or UHF-unstable correction^b	BAC-MP2	BAC-MP3	BAC-MP4 (SDQ)	BAC-MP4 (SDTQ)
^{1}SbH	100.39	10.15 u	84.71	83.33	82.52	82.28
^{3}SbH	67.78	0.59 s	59.42	59.59	59.28	59.26
Sb(H)$_2$	67.24	0.54 s	50.76	50.91	50.67	50.64
Sb(H)$_3$	61.01		36.63	36.62	36.62	36.62
^{1}Sb(CH$_3$)	107.08	10.15 u	77.71	76.63	75.71	75.40
^{3}Sb(CH$_3$)	76.01	0.66 s	54.19	54.49	54.01	54.04
Sb(CH$_3$)$_2$	81.80	0.58 s	38.46	38.68	38.26	38.31
Sb(CH$_3$)$_3$	79.76		15.25	14.90	14.82	15.03
Sb(H)(CH$_3$)	75.19	0.57 s	45.29	45.47	45.11	45.16
Sb(H)$_2$(CH$_3$)	68.60		30.86	30.75	30.69	30.81
Sb(H)(CH$_3$)$_2$	74.85		23.74	23.50	23.42	23.61
^{1}Sb(C$_2$H$_5$)	118.89	10.15 u	76.47	76.36	75.61	74.60
^{3}Sb(C$_2$H$_5$)	87.37	0.73 s	52.46	53.51	53.19	52.61
Sb(C$_2$H$_5$)$_2$	104.10	0.62 s	34.65	36.56	36.52	35.16
Sb(C$_2$H$_5$)$_3$	112.64		9.00	11.22	11.76	9.79
Sb(H)(C$_2$H$_5$)	86.33	0.60 s	43.36	44.29	44.12	43.55
Sb(H)$_2$(C$_2$H$_5$)	79.72		28.93	29.57	29.71	29.22
Sb(H)(C$_2$H$_5$)$_2$	96.82		19.59	21.00	21.34	20.15
^{1}SbCl	67.84	10.15 u	45.15	44.08	43.25	42.68
^{3}SbCl	37.87	0.59 s	22.96	22.96	22.66	22.77
Sb(Cl)$_2$	7.31	0.47 s	−23.12	−23.10	−23.38	−23.26
Sb(Cl)$_3$	−28.30		−74.68	−74.84	−74.85	−74.57
Sb(H)(Cl)	39.21	0.50 s	16.26	16.12	15.86	16.08
Sb(H)$_2$(Cl)	34.89		4.04	3.58	3.60	4.00
Sb(H)(Cl)$_2$	5.05		−33.23	−33.77	−33.74	−33.24
Sb(CH$_3$)(Cl)	43.40	0.52 s	7.11	7.11	6.77	7.01
Sb(CH$_3$)$_2$(Cl)	41.32		−16.21	−16.69	−16.70	−16.21
Sb(CH$_3$)(Cl)$_2$	5.30		−46.22	−46.64	−46.64	−46.12
^{1}Sb(OH)	51.12	10.05 u	20.20	21.15	18.85	17.28
^{3}Sb(OH)	29.87	0.55 s	6.26	7.21	6.35	6.09
Sb(OH)$_2$	−17.44	0.46 s	−64.56	−63.67	−64.50	−64.77
Sb(OH)$_3$	−78.74		−149.26	−150.04	−150.04	−149.77
Sb(H)(OH)	29.65	0.48 s	−1.88	−1.14	−1.93	−2.17
Sb(H)$_2$(OH)	23.87		−15.27	−15.61	−15.72	−15.55
Sb(H)(OH)$_2$	−23.15		−77.78	−78.30	−78.49	−78.30
Sb(CH$_3$)(OH)	34.01	0.50 s	−11.02	−10.43	−11.29	−11.38
Sb(CH$_3$)$_2$(OH)	30.94		−35.23	−35.69	−36.02	−35.73
Sb(CH$_3$)(OH)$_2$	−21.27		−89.60	−89.90	−90.46	−90.32
Sb(Cl)(OH)	−6.04	0.47 s	−44.51	−43.98	−44.59	−44.68
Sb(Cl)$_2$(OH)	−47.34		−101.50	−101.70	−101.80	−101.56
Sb(Cl)(OH)$_2$	−64.26		−126.44	−126.90	−126.99	−126.75
Sb(H)$_2$(CH$_2$)	115.13	1.13 s	79.90	78.87	79.01	79.84
Sb(H)$_2$(O)	75.55	1.06 s	48.47	45.83	45.94	46.20
ax-Sb(Cl)$_3$(H)	18.70	1.45 s	−33.90	−32.59	−32.61	−32.52
trans-ax-Sb(Cl)$_3$(H)$_2$	26.22		−38.35	−37.82	−37.22	−36.10
cis-eq-Sb(Cl)$_3$(H)$_2$	23.48		−41.00	−40.77	−40.08	−38.50
ax-Sb(Cl)$_4$	−8.96	1.86 s	−69.06	−67.59	−67.91	−68.13
eq-Sb(Cl)$_4$	−9.59	1.56 s	−70.34	−69.5	−69.81	−69.41
ax-Sb(Cl)$_4$(H)	1.95		−70.82	−70.92	−70.64	−69.42
eq-Sb(Cl)$_4$(H)	0.73		−71.95	−72.22	−71.91	−70.33
Sb(Cl)$_5$	−23.32		−104.05	−104.38	−104.42	−103.03

^{a} All values in kcal/mol. ^{b} u, UHF-unstable correction; s, spin-contamination correction. Spin contamination is the spin contamination contribution of excited states into the ground state that is present in open-shell molecules calculated using the UHF method.

TABLE 4: BAC-MP4 $\Delta H_f°$(298 K) and Corresponding Literature Values^a

	BAC-MP4^b	literature	ref
Sb(H)$_3$	34.6 ± 1.0	34.681	20
Sb(CH$_3$)$_3$	9.2 ± 1.0	7.4 ± 3.2	23
		9.2	22
		7.7 ± 6.0	21
Sb(C$_2$H$_5$)$_3$	−0.2 ± 2.6	13.1	24
		11.6 ± 2.6	21
^{3}SbCl	22.6 ± 1.0	−6.22	20
Sb(Cl)$_2$	−23.6 ± 1.0	−18.5	20
Sb(Cl)$_3$	−74.9 ± 1.1	−75.0	20

^{a} All values in kcal/mol. ^{a} BAC-MP4 errors estimated using eq 7.

containing antimony compounds. Thus, the heat of formation of Sb(CH$_3$)(H)$_2$ was calculated and compared to the BAC-MP4

value to test the Sb−C bond correction. The CCSD(T) heat of formation at 298 K is 27.2 kcal/mol, and the BAC-MP4 value is 27.3 kcal/mol, an agreement that gives confidence in the Sb−C bond correction and the literature Sb(CH$_3$)$_3$ heat of formation upon which it is based.

The literature $\Delta H_f°$(298 K) value for Sb(C$_2$H$_5$)$_3$, 11.6 ± 2.6 kcal/mol,[21] is more positive than that obtained from the BAC-MP4 method, −0.2 ± 2.6 kcal/mol. Gmelin proposes another heat of formation value, 13.1 kcal/mol, although the error limits of this calculation are not reported.[24] The agreement between the CCSD(T) heat of formation of Sb(CH$_3$)(H)$_2$ and the Sb(CH$_3$)$_3$-calibrated BAC-MP4 heat of formation for this compound and our previous finding that calibrating M−C bonds with methyl species works well for molecules containing longer-chain alkane ligands[19] support the use of Sb(CH$_3$)$_3$ to calibrate

TABLE 5: $\Delta H_f°$(298 K) (with Errors), $\Delta S°$(298 K), and $\Delta G_f°(T)$ Derived from BAC-MP4 Calculations[a]

	$\Delta H_f°$(298 K)[b]	$\Delta S°$(298 K)	$\Delta G_f°$(T/K)					
			300	600	1000	1500	2000	2500
^{1}SbH	81.9 ± 2.5	49.42	75.0	68.5	60.7	53.8	47.1	39.4
^{3}SbH	58.9 ± 1.1	51.61	51.3	44.1	35.5	27.5	19.7	10.9
Sb(H)$_2$	49.6 ± 1.0	55.99	45.3	41.7	37.9	35.9	34.0	31.0
Sb(H)$_3$	34.6 ± 1.0	55.58	35.1	36.5	39.4	45.4	51.4	56.1
^{1}Sb(CH$_3$)	73.3 ± 2.6	63.39	72.0	71.4	72.2	76.2	80.5	83.4
^{3}Sb(CH$_3$)	51.9 ± 1.1	65.38	49.9	48.8	49.0	52.2	55.6	57.7
Sb(CH$_3$)$_2$	34.4 ± 1.1	79.32	42.6	52.2	67.3	89.4	111.5	132.0
Sb(CH$_3$)$_3$	9.2 ± 1.0	88.80	29.0	50.6	82.1	124.6	166.8	206.9
Sb(H)(CH$_3$)	42.5 ± 1.1	68.44	44.2	47.0	52.4	62.1	71.9	80.3
Sb(H)$_2$(CH$_3$)	27.3 ± 1.0	68.33	33.7	41.3	53.2	70.7	88.0	103.8
Sb(H)(CH$_3$)$_2$	18.8 ± 1.0	78.67	31.9	46.5	68.2	98.2	127.9	155.9
^{1}Sb(C$_2$H$_5$)	71.1 ± 3.0	72.46	76.7	83.6	94.9	112.2	129.5	145.3
^{3}Sb(C$_2$H$_5$)	49.0 ± 1.5	73.75	54.2	60.7	71.4	88.0	104.6	119.6
Sb(C$_2$H$_5$)$_2$	28.3 ± 2.2	94.60	51.4	76.5	112.7	160.7	208.0	252.8
Sb(C$_2$H$_5$)$_3$	−0.2 ± 2.6	113.18	41.5	85.8	148.6	230.4	311.3	389.2
Sb(H)(C$_2$H$_5$)	39.4 ± 1.4	76.96	48.4	58.6	74.4	97.0	119.6	140.5
Sb(H)$_2$(C$_2$H$_5$)	24.2 ± 1.2	76.72	37.9	53.0	75.2	105.6	135.7	163.9
Sb(H)(C$_2$H$_5$)$_2$	12.5 ± 1.8	94.12	40.4	70.3	113.0	169.1	224.4	277.1
^{1}SbCl	42.5 ± 2.7	59.25	35.9	29.7	22.1	15.4	9.1	1.7
^{3}SbCl	22.6 ± 1.0	61.5	15.3	8.4	0.0	−7.9	−15.4	−23.9
Sb(Cl)$_2$	−23.6 ± 1.0	74.57	−26.8	−29.7	−33.0	−34.4	−35.6	−37.9
Sb(Cl)$_3$	−74.9 ± 1.1	81.46	−72.2	−69.4	−65.4	−58.0	−50.7	−44.6
Sb(H)(Cl)	15.2 ± 1.0	66.82	11.0	7.3	3.2	0.8	−1.5	−4.8
Sb(H)$_2$(Cl)	2.3 ± 1.2	66.77	2.7	3.8	6.2	11.5	16.8	20.8
Sb(H)(Cl)$_2$	−34.4 ± 1.2	75.43	−33.2	−31.7	−28.9	−23.2	−17.5	−13.0
Sb(CH$_3$)(Cl)	4.9 ± 1.0	77.67	7.2	10.3	15.9	25.9	36.0	44.7
Sb(CH$_3$)$_2$(Cl)	−20.2 ± 1.2	87.23	−6.4	8.7	30.7	61.1	91.2	119.6
Sb(CH$_3$)(Cl)$_2$	−48.3 ± 1.2	85.4	−40.3	−31.7	−19.1	−0.8	17.3	34.0
^{1}Sb(OH)	16.3 ± 4.7	60.59	13.3	10.9	8.6	8.5	8.8	8.0
^{3}Sb(OH)	5.1 ± 1.5	62.91	1.5	−1.7	−5.0	−6.3	−7.3	−9.3
Sb(OH)$_2$	−66.7 ± 1.5	74.98	−62.0	−56.8	−49.0	−36.7	−24.3	−12.9
Sb(OH)$_3$	−152.6 ± 1.1	81.44	−137.8	−122.7	−102.3	−74.5	−47.0	−20.9
Sb(H)(OH)	−3.7 ± 1.5	66.47	−3.8	−3.2	−1.5	3.4	8.4	12.4
Sb(H)$_2$(OH)	−18.1 ± 1.0	65.64	−13.3	−7.7	0.6	13.4	26.1	37.4
Sb(H)(OH)$_2$	−81.1 ± 1.0	73.83	−71.4	−61.0	−46.5	−26.0	−5.6	13.4
Sb(CH$_3$)(OH)	−14.3 ± 1.4	77.47	−7.9	−0.6	10.8	28.0	45.4	61.3
Sb(CH$_3$)$_2$(OH)	−40.5 ± 1.0	87.56	−22.7	−3.6	23.9	61.2	98.3	133.5
Sb(CH$_3$)(OH)$_2$	−94.2 ± 1.1	84.41	−77.9	−60.7	−36.5	−3.7	28.9	59.9
Sb(Cl)(OH)	−45.7 ± 1.2	76.29	−45.4	−44.7	−42.9	−38.1	−33.1	−29.2
Sb(Cl)$_2$(OH)	−102.8 ± 1.0	82.83	−96.5	−90.0	−81.0	−67.5	−54.1	−41.9
Sb(Cl)(OH)$_2$	−128.9 ± 1.0	82.28	−118.4	−107.4	−92.2	−70.9	−49.5	−29.5
Sb(H)$_2$(CH$_2$)	77.3 ± 1.6	70.41	78.5	80.4	84.2	91.6	99.0	104.9
Sb(H)$_2$(O)	44.4 ± 1.1	65.18	44.7	45.6	47.6	52.4	57.1	60.5
ax-Sb(Cl)$_3$(H)	−33.9 ± 1.0	89.06	−28.8	−23.3	−15.2	−2.6	10.0	21.4
*trans-ax-*Sb(Cl)$_3$(H)$_2$	−38.1 ± 2.3	85.13	−27.2	−15.9	−0.4	20.7	41.3	60.2
*cis-eq-*Sb(Cl)$_3$(H)$_2$	−40.5 ± 2.9	85.96	−29.8	−18.8	−3.9	16.6	36.6	55.0
ax-Sb(Cl)$_4$	−68.6 ± 1.2	94.7	−61.9	−55.1	−45.6	−31.4	−17.1	−4.0
eq-Sb(Cl)$_4$	−69.5 ± 1.1	97.47	−63.6	−57.8	−50.2	−38.7	−27.6	−17.8
ax-Sb(Cl)$_4$(H)	−70.6 ± 2.2	94.47	−59.2	−47.7	−32.4	−11.4	9.0	27.7
eq-Sb(Cl)$_4$(H)	−71.5 ± 2.7	92.02	−59.4	−47.2	−30.9	−8.9	12.6	32.4
Sb(Cl)$_5$	−103.5 ± 2.2	100.86	−90.7	−78.1	−61.6	−39.5	−17.8	2.2

[a] Energies in kcal/mol, entropies in cal/mol·K. [b] BAC-MP4 errors estimated using eq 7.

the Sb−C bond and suggest that the reported experimental value might be higher than the true value.

$\Delta H_f°$(298 K) values of the SbCl$_n$, $n = 1-3$, series are reported in the NBS tables[20] without an experimental reference or error estimates. SbCl$_3$ was used to calibrate the Sb−Cl BAC correction in this study, and the literature $\Delta H_f°$(298 K) for SbCl$_2$ is −18.5 kcal/mol, 5.1 kcal/mol greater than the BAC-MP4 value of −23.6 ± 1.1 kcal/mol. The difference between calculated and literature heats of formation for SbCl is even greater, with the NBS tables proposing −6.22 kcal/mol (presumably for the lower-energy triplet state) while the corresponding BAC-MP4 value is 22.6 kcal/mol. In the absence of an experimental method, the origin of these differences cannot be explored.

Table 5 provides the heats of formation, $\Delta H_f°$(298 K); entropies, $S°$(298 K); and Gibbs free energies of formation, $\Delta G_f°$(298 K), for the 51 molecules investigated in this study, and CHEMKIN-compatible polynomial fits[29] of C_p, $S°$, and the enthalpy functions for each compound can be found in the Supporting Information and on the Internet.[30] Bond dissociation energies derived from the BAC-MP4-calculated $\Delta H_f°$(298 K) values for the compounds, A−B, A, and B in the reaction A−B → A + B are found in Table 6.

III.3. $\Delta H_f°$ vs Ligand Substitution. Variation in the heat of formation upon ligand substitution is of interest to CVD precursor selection as it allows precursors of varying stability to be chosen depending on the experimental conditions. Figure 1 shows that the decrease in $\Delta H_f°$(298 K) upon substituting
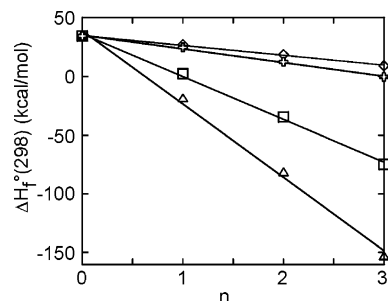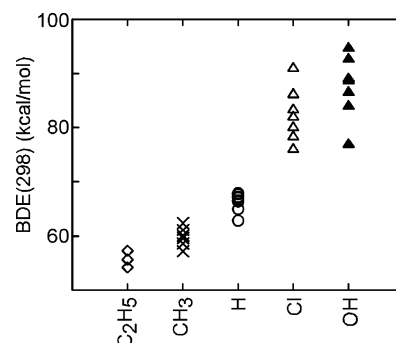
TABLE 6: Sb−L Bond Dissociation Energies (BDEs) at 298 K (kcal/mol)

	ΔH$_f$°(298 K) BAC-MP4 (SDTQ)	BDE			
		Sb−H	Sb−C	Sb−Cl	Sb−O
^{1}SbH	81.9	32.9			
^{3}SbH	58.9	55.9			
$Sb(H)_2$	49.6	61.4			
$Sb(H)_3$	34.6	67.1			
$^1Sb(CH_3)$	73.3		24.3		
$^3Sb(CH_3)$	51.9		45.7		
$Sb(CH_3)_2$	34.4		52.4		
$Sb(CH_3)_3$	9.2		60.1		
$Sb(H)(CH_3)$	42.5	61.5	51.3		
$Sb(H)_2(CH_3)$	27.3	67.3	57.2		
$Sb(H)(CH_3)_2$	18.8	67.7	58.6		
$^1Sb(C_2H_5)$	71.1		24.9		
$^3Sb(C_2H_5)$	49.0		47.0		
$Sb(C_2H_5)_2$	28.3		49.5		
$Sb(C_2H_5)_3$	−0.2		57.3		
$Sb(H)(C_2H_5)$	39.4	61.7	48.3		
$Sb(H)_2(C_2H_5)$	24.2	67.3	54.2		
$Sb(H)(C_2H_5)_2$	12.5	67.9	55.7		
^1SbCl	42.5			49.2	
^3SbCl	22.6			69.1	
$Sb(Cl)_2$	−23.6			75.2	
$Sb(Cl)_3$	−74.9			80.3	
$Sb(H)(Cl)$	15.2	59.5		72.7	
$Sb(H)_2(Cl)$	2.3	65.0		76.3	
$Sb(H)(Cl)_2$	−34.4	62.9		78.6	
$Sb(CH_3)(Cl)$	4.9		52.6	76.0	
$Sb(CH_3)_2(Cl)$	−20.2		60.0	83.6	
$Sb(CH_3)(Cl)_2$	−48.3		59.6	82.2	
$^1Sb(OH)$	16.3				55.8
$^3Sb(OH)$	5.1				67.0
$Sb(OH)_2$	−66.7				81.2
$Sb(OH)_3$	−152.6				95.0
$Sb(H)(OH)$	−3.7	61.0			72.1
$Sb(H)_2(OH)$	−18.1	66.4			77.1
$Sb(H)(OH)_2$	−81.1	66.6			86.8
$Sb(CH_3)(OH)$	−14.3		54.3		75.6
$Sb(CH_3)_2(OH)$	−40.5		61.1		84.3
$Sb(CH_3)(OH)_2$	−94.2		62.4		89.3
$Sb(Cl)(OH)$	−45.7			79.8	77.7
$Sb(Cl)_2(OH)$	−102.8			86.4	88.9
$Sb(Cl)(OH)_2$	−128.9			91.5	92.9
$ax\text{-}Sb(Cl)_3(H)$	−33.9		11.1	28.5	
$trans\text{-}ax\text{-}Sb(Cl)_3(H)_2$	−38.1		56.3		
$cis\text{-}eq\text{-}Sb(Cl)_3(H)_2$	−40.5		58.7		
$ax\text{-}Sb(Cl)_4$	−68.6			22.7	
$eq\text{-}Sb(Cl)_4$	−69.5			23.6	
$ax\text{-}Sb(Cl)_4(H)$	−70.6		54.1	65.7	
$eq\text{-}Sb(Cl)_4(H)$	−71.5		54.1	66.6	
$Sb(Cl)_5$	−103.5			63.9 (ax) 63.0 (eq)	

	ΔH$_f$°(298 K) BAC-MP4(SDTQ)	R−H BDE
$(H)_2SbCH_2$−H	27.3	102.1
$(H)_2SbO$−H	−18.1	114.6

Figure 1. Heats of formation (298 K) for $SbH_{3-n}X_n$ [$n = 0-3$; X = OH (△), Cl (□), CH_3 (◇), C_2H_5 (+)]. All converge at SbH_3 (i.e., $n = 0$, $3 - n = 3$).

Figure 2. Bond dissociation energies (BDEs) for three-coordinate compounds of the form YZSb−X. X is denoted on the horizontal axis.

Sb−Y bond. A negative gradient, as is observed for OH, Cl, C_2H_5, and CH_3 upon substitution for H in Figure 1, indicates that the Sb−H bond delivers the least enthalpic stabilization of the ligands under investigation.

Elements adjacent to Sb in the fourth row of the periodic table, indium[18] and tin,[19] show similar behavior upon ligand substitution; σ-acceptor ligands, such as H, show little deviation from linearity, whereas σ-acceptor, π-donor ligands, such as OH and Cl, show a larger deviation. This nonlinearity has been ascribed to multiple metal−ligand bonds drawing upon the same metal orbitals [e.g., the M−A and M−B bonds of the molecule A−M−B both drawing upon the M(p$_x$) atomic orbital].[19] Considering the $MCl_n(CH_3)_{3-n}$ (M = Sb, In) and $SnCl_n(CH_3)_{4-n}$ series, the nonlinearity is smallest for Sb, intermediate for Sn, and greatest for In compounds.

In a parallel, previous investigation,[18] indium compounds of the form InXYZ (where X, Y, and Z are the ligands investigated in the present study) were found to display a linear variation in heat of formation upon ligand substitution (e.g., for InXY$_2$, InXYZ, and InXZ$_2$). Additionally, the change in the heat of formation upon ligand substitution is similar to that of the $InY_{3-n}Z_n$ ($n = 0-3$) series. Assuming that the same relationships are valid for Sb compounds, this observation greatly expands the number of molecules whose thermochemistry can be explored using the data of Table 5, albeit with a larger uncertainty than for species that are calculated explicitly. Such a parallel is anticipated as the heats of formation of the $InY_{3-n}Z_n$ ($n = 0-3$), $SnY_{4-n}Z_n$ ($n = 0-4$), and $SbY_{3-n}Z_n$ ($n = 0-3$) series display a near-linear variation with n.

III.4. Bond Dissociation Energies (BDEs). Of great interest to the modeling of CVD gas-phase reaction chemistry is the bond dissociation energy (BDE), the energy required to split a molecule A−B into neutral fragments A and B. These data for the Sb−H−C−O−Cl system are collected in Table 6 and are represented graphically in Figure 2. The trend in BDE is BDE(Sb−C_2H_5) < BDE(Sb−CH_3) < BDE(Sb−H) < BDE(Sb−

CH$_3$, C$_2$H$_5$, OH, or Cl for H in the series $SbH_{3-n}X_n$ ($n = 0-3$) is monotonic and nearly linear. For molecules with a small change in ΔH$_f$°(298 K) upon substitution, there is a slight deviation from linearity, whereas for ligands with a larger ΔH$_f$°(n) gradient, such as OH and Cl, the deviation is greater, as can be seen in Figure 1 (the $n = 1$ and 2 data points are above the line of best fit, whereas the $n = 0$ and 3 data are below). Other series of the form SbX_nY_{3-n} also display a deviation from linearity that increases with the difference between the heat of formation of the SbX_3 and SbY_3 compounds. The ΔH$_f$°(n) gradient for SbX_nY_{3-n} reflects the difference in molecular enthalpic stabilization due to an Sb−X versus an
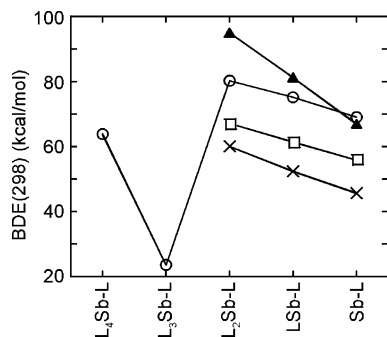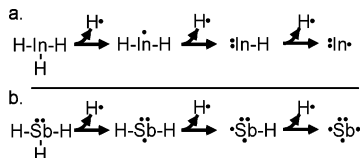
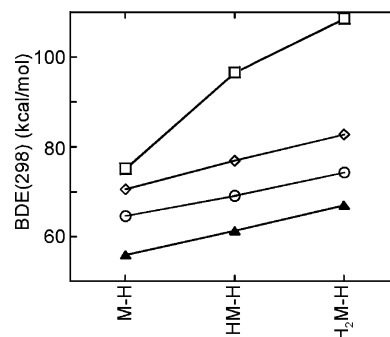**Figure 3.** Bond dissociation energies (BDEs) for SbL_n compounds [L = H ($\square$), CH_3 ($\times$), Cl ($\bigcirc$), OH ($\triangle$); $n = 1-5$].

Figure 4. Lewis dot structures for the successive hydrogen-atom removal from (a) InH_3 and (b) SbH_3.

Cl) < BDE(Sb−OH). This trend is similar to that calculated for InL_3 compounds using the same ligand set, except that the −Cl BDEs are, on average, greater than the −OH BDEs for InL_3, albeit with a large degree of overlap. This difference might be due to the different electronic structures of indium and antimony molecules. The average BDE of XYIn−OH is 88.2 kcal/mol, that of XYSb−OH is 87.8 kcal/mol, that of XYIn−Cl is 93.7 kcal/mol, and that of XYSb−Cl is 82.7 kcal/mol. The XYM−OH BDEs differ by only 0.4 kcal/mol, whereas those of XYM−Cl differ by 11.0 kcal/mol, indicating that differences in the nature of the M−Cl bond are the source of the difference in the BDE trend. OH is a σ-accepting, weakly π-donating ligand, whereas Cl is σ-accepting, π-donating. Indium in ML_3 compounds is a σ-donor, π-acceptor because of the empty $5p_z$ orbital, allowing the formation of a strong In−Cl bond, whereas antimony is a σ-donor that cannot participate in back-bonding because its 5s and 5p orbitals are filled, resulting in a relatively weak Sb−Cl bond and the observed BDE trends.

For In, it was found that substitution of methoxide, OCH_3, for OH ligands resulted in a smaller BDE by 9 kcal/mol for equivalent indium compounds.[18] Similarly, BDEs for indium−ethyl bonds were less than those with methyl ligands. The same trend was observed for Sb−C_2H_5 vs Sb−CH_3 BDEs, suggesting that Sb−OCH_3 BDEs will be less than those of equivalent Sb−OH-containing molecules.

III.5. Successive Ligand Elimination. The BDEs for successive ligand dissociation are important for gas-phase pyrolysis reactions during CVD processes. For antimony, the calculated successive BDEs for ML_3, ML_2, and ML decrease monotonically (Table 6, Figure 3). This is in contrast to group III and IV compounds, such as indium[18] and tin,[19] for which a "high−low−high" BDE pattern known as the "inert-pair effect",[61] is observed. This difference might be due to the differing electronic structures of these compounds. The inert-pair effect is attributed to the larger splitting of the s and p electronic levels with increasing atomic number, resulting in the s electrons playing a smaller role in bonding and acting as an "inert pair" of electrons. For indium, this 5s electron pair is called upon for the formation of the second In−H bond in InH_2 (Figure 4a), resulting in a relatively weak bond and low BDE relative to those of InH and InH_3. In contrast, atomic antimony has three

electrons distributed among its 5p orbitals (Figure 4b), each of which can donate an electron to a bonding orbital with H•. As a result, a smoother, near-linear variation in BDE is observed with the breaking of each successive Sb−H bond.

However, the Sb−Cl BDEs of the $SbCl_n$, $n = 5-3$, group (63.0, 23.6, and 80.3 kcal/mol, respectively) display the high−low−high pattern also exhibited by the tin (SnL_n, $n = 2-4$) and indium (InL_n, $n = 1-3$) triads (Table 6, Figure 3). This is because the addition of a fourth metal−ligand bond to antimony involves the low-lying 5s orbital, creating a less stable bond and a lower calculated BDE. It is striking that the inert-pair effect is observed across such a broad range of coordination numbers and molecular geometries, depending on the atomic number of the central metal atom and resulting electronic structure of the resulting molecules.

For group V elements, the BDE trend for ML_3, ML_2, and ML is difficult to determine from experimental data because of a paucity of such complete information for any metal−ligand pair. The only reported experimental data for antimony is the $SbCl_n$ series, found in the NBS tables, which provide only thermodynamic values, not the manner in which they were derived.[20] The values given are 85.5, 41.3, and 97.9 kcal/mol for the Sb−Cl BDEs of $SbCl_3$, $SbCl_2$, and SbCl, respectively, giving the high−low−high pattern observed for groups III and IV molecules. However, in the absence of an experimental literature reference, the veracity of this claim cannot be verified. The greatest body of experimental group V data is available for phosphorus the species (PH_n,[34] PF_n,[34,55] and PCl_n[55]), which display a near-linear BDE progression, paralleling the trend calculated for Sb, rather than the high−low−high progression of group III and IV molecules.[18,19] The NH_n BDE trend is similarly linear. These observations are reproduced by G2 calculations for MH_n, (M = N, P, As; $n = 1-3$), as shown in Figure 5, and reinforce the concept that trends in bonding and thermodynamic properties are dominated by the electronic structure of the molecules, making comparisons within groups of the periodic table much more fruitful than those across its rows.

III.6. Additional Precursor Decomposition Mechanisms. In addition to sequential ligand dissociation, a variety of gas-phase reaction mechanisms can be employed in MOCVD precursor decomposition. Among these are β-hydride elimination and molecular elimination reactions. These reactions are important in the environment of a CVD reactor because the reactant concentrations are low, making reactions that require no intermolecular collisions more prevalent. Sequential ligand elimination from SbL_3 results in the release of two coordinatively unsaturated radical molecules, L•, that are often unstable relative to the L_2 molecule. The thermodynamically more

Figure 5. Bond dissociation energies (BDEs) for group V compounds MH_n [M = N ($\square$), P ($\diamondsuit$), As ($\bigcirc$), Sb ($\blacktriangle$); $n = 1-3$]. N, P, and As BDEs are from G2 calculations;[62] Sb BDEs are from this work.

favored reaction product is determined by the temperature of the system, with the enthalpic stabilization of bond formation predominating at lower temperatures, whereas the entropic driving force favors the generation of additional molecules at higher temperatures. At typical CVD temperatures (200−600 °C) the L_2 species is more stable for each of the five ligands explored in this study (the first L_2 molecule to thermally cleave is H_2O_2, which dissociates to form 2OH• above ~1650 K).[30] However, flow-tube decomposition experiments suggest that the primary decomposition mechanism for trimethylantimony is radical elimination,[15] with the resulting methyl radicals abstracting a hydrogen atom from $Sb(CH_3)_3$ to form methane and $Sb(CH_3)_2(CH_2)$.[17]

Similarly, β-hydride elimination is a radical-free precursor decomposition mechanism that can occur for molecules containing hydrocarbon ligands with more than one carbon. This mechanism is of particular interest, as it often results in low-carbon impurities in the resulting deposited films,[1] although it was found to be a minor contributor to $As(C_2H_5)_3$ pyrolysis[63] and $Sb(i\text{-}C_3H_7)_3$ decomposes via a radical mechanism.[14] Kinetics, especially the energetics of the transition state, determines which of these reactions (radical elimination, molecular elimination, β-hydride elimination, or some other mechanism) will be observed and is beyond the scope of the current work.

III.7. Ligand Decomposition: $Sb(H)_2CH_2$ and $Sb(H)_2O$. In addition to ligand elimination via the breaking of an Sb−L bond, metal−organic precursors can pyrolize via ligand decomposition. This can occur either through a unimolecular decomposition reaction or through atom abstraction by a radical such as a previously eliminated methyl ligand, CH_3• (vide supra). To investigate such reactions, the hydrogen-atom-elimination reaction products of $Sb(H)_2CH_3$ and $Sb(H)_2OH$, namely, $Sb(H)_2CH_2$ and $Sb(H)_2O$, respectively, were calculated via the BAC-MP4 method. Both reactions were calculated to be highly endothermic (and are the same as the corresponding R−H BDE reactions), by 102.1 and 114.6 kcal/mol at 298 K (calculated from Table 5), and to be nonspontaneous ($\Delta G°_{rxn} < 0$) at temperatures below 2500 K (the highest temperature for which $\Delta G°$ was calculated in this study). In addition, the C−H BDE, 102.1 kcal/mol, is much greater than the Sb−H (67.3 kcal/mol) and Sb−C (57.2 kcal/mol) BDEs of $Sb(H)_2CH_3$, suggesting that these bonds would break preferentially. Similarly, the O−H BDE, 114.6 kcal/mol, is much greater than the Sb−H (66.4 kcal/mol) and Sb−O (77.2 kcal/mol) BDEs of $Sb(H)_2OH$, although for $Sb(OH)_3$, the Sb−O BDE is 95.0 kcal/mol, approaching the O−H BDE of $Sb(H)_2OH$.

The second decomposition mechanism, radical abstraction, is expected to be more enthalpically favored because it involves the stabilization of a radical reactant. Hydrogen-atom abstraction by methyl radical is identified as an important reaction step in trimethyl antimony decomposition to give methane and $Sb(CH_3)_2(CH_2)$.[17] The equivalent reaction of CH_3• with $Sb(H)_2CH_3$ to form $Sb(H)_2CH_2$ and methane is calculated to be slightly exothermic (−2.8 kcal/mol) and is spontaneous below 875 K, supporting the experimental observation. Of course, methyl-radical attack on $Sb(H)_2CH_3$ thermodynamically favors cleavage of the Sb−H bond to form $Sb(H)CH_3$ and methane, as the Sb−H bond is much weaker than the C−H bond (Table 5). This is consistent with the finding that $Sb(H)(i\text{-}C_3H_7)_2$ decomposes to give $Sb(i\text{-}C_3H_7)$ and propane,[16] which might arise from a unimolecular isopropyl-radical elimination step, followed by abstraction of the hydrogen ligand by this radical.

Although longer-chain alkyl ligands have not been considered in this study, the C−H bond strengths of $Sn(H)_3CH_3$ and $Sb(H)_3CH_3$ are quite similar (102.5[19] and 102.1 kcal/mol, respectively). Thus, it might be reasonable to assume that the C−H bond energies for such antimony species will mirror those of tin compounds, with internal C-H bonds (e.g., α-H of butyl ligands) being weaker than terminal C−H bonds.[19]

III.8. Four- and Five-Coordinate Molecules: $Sb(H)_x(Cl)_y$ and $Sb(Cl)_z$. Ligand addition to three-coordinate antimony compounds can also occur in the gas phase. Such reactions are considered because five-coordinate compounds of group V elements, such as PCl_5, are well-known. Addition of one or two water ligands to SbH_3 was found to be unstable relative to the starting reactants. This is in contrast to water addition to indium complexes, such as $In(CH_3)_3$, to form $In(CH_3)_3(H_2O)_2$, which is calculated to be exothermic at 298 K.[18] This difference arises because SbL_3 contains a lone pair, which repels the electron-donating water molecule, in contrast to $In(CH_3)_3$, which has an unoccupied $5p_z$ orbital.

However, addition of two open-shell ligands, such as Cl•, to an SbL_3 molecule, such as $SbCl_3$, to form $Sb(Cl)_5$ might be stable, by extension from PCl_5. Thus, the thermochemistry of the geometric isomers of five-coordinate molecules $Sb(Cl)_5$, $Sb(Cl)_4(H)$, and $Sb(Cl)_3(H)_2$ and their four-coordinate elimination products was investigated (Tables 3, 5, and 6).[57] The addition of Cl• to $Sb(Cl)_3$ at 298 K to form $Sb(Cl)_4$ was calculated to be exothermic by 23.6 kcal/mol, and the addition of a second Cl atom was found to be further exothermic by 63.0 kcal/mol. Cl_2 is more stable than 2Cl• at 298 K, but the direct addition of Cl_2 to form $Sb(Cl)_5$ is still exothermic by 28.6 kcal/mol. This molecular addition reaction was calculated to be spontaneous below 875 K. In contrast, the addition of H_2 to $Sb(Cl)_3$ at 298 K is endothermic by 34.4 kcal/mol because of the larger enthalpic penalty of breaking a H−H bond than a Cl−Cl bond and the larger Sb−Cl versus Sb−H BDEs.

A small energetic difference was calculated for geometric isomers of $Sb(Cl)_4(H)$ and $Sb(Cl)_3(H)_2$ depending on whether the hydrogen atoms are located in the equatorial or axial positions of the trigonal bipyramid. The isomer of $Sb(Cl)_4(H)$ with H in the equatorial position is 0.9 kcal/mol more stable than $ax\text{-}Sb(Cl)_4(H)$. Similarly, $eq\text{-}Sb(Cl)_3(H)_2$ (both H atoms in the equatorial positions) is 1.4 kcal/mol more stable than $ax\text{-}Sb(Cl)_3(H)_2$. The isomer with one hydrogen in an axial and the other in an equatorial coordination converted to $eq\text{-}Sb(Cl)_3(H)_2$ during the geometry optimization step of the MP4 calculation, indicating a near-barrierless interconversion. For both $Sb(Cl)_4(H)$ and $Sb(Cl)_3(H)_2$, interconversion via a low-energy-barrier Berry pseudorotation (a ~35 kcal/mol barrier was calculated for PF_5[64]) between these isomers might occur at typical CVD temperatures (300−600 K).

IV. Summary and Conclusions

Motivated by the need for thermochemical data for choosing metal−organic precursors for CVD of antimony-containing thin films, a wide range of thermochemical data have been calculated using the BAC-MP4 methodology. This approach was calibrated by a combination of experimental data and high-level coupled-cluster calculations. The 51 SbL_n (L = H, CH_3, C_2H_5, Cl, and OH; $n = 1−5$) molecules form a basis for evaluating the thermodynamic behavior of a range of alkyl-, chloro-, and hydroxostibines using both the data provided herein and interpolation based on trends discernible in the predicted heats of formation. Linear variation in heats of formation upon ligand substitution, trends in BDEs with ligand identity [BDE(Sb−C_2H_5) < BDE(Sb−CH_3) < BDE(Sb−H) < BDE(Sb−Cl) < BDE(Sb−OH)], and a monotonic decrease in BDE upon

successive ligand elimination were identified. These results were contrasted to those of other group V (N, P, As) and fourth row (In, Sn) compounds, revealing greater similarity within group V. The thermochemical data are consistent with those from previous studies[19,25−28,30,48−51,65] and can aid in the selection of CVD precursors and deposition conditions for the formation of antimony-containing materials, as well as in understanding the chemistry of antimony in general.

Supporting Information Available: Tables listing molecular geometries, vibrational data, and Chemkin coefficients. This material is available free of charge via the Internet at http://pubs.acs.org.

References and Notes

(1) Schulz, S. *Coord. Chem. Rev.* **2001**, *215*, 1.

(2) Biefeld, R. M.; Kurtz, S. R.; Fritz, I. J. *J. Electron. Mater.* **1989**, *18*, 775.

(3) Stradling, R. A. *Semicond. Sci. Technol.* **1991**, *6*, C52.

(4) Egan, R. J.; Chin, V. W. L.; Tansley, T. L. *Semicond. Sci. Technol.* **1994**, *9*, 1591.

(5) Wang, C. A.; Jensen, K. F.; Jones, A. C.; Choi, H. K. *Appl. Phys. Lett.* **1996**, *68*, 400.

(6) Samoska, L. A.; Brar, B.; Kroemer, H. *Appl. Phys. Lett.* **1993**, *62*, 2539.

(7) Zhang, Y.; Baruch, N.; Wang, W. I. *Appl. Phys. Lett.* **1993**, *63*, 1068.

(8) Leroux, M.; Tromsoncarli, A.; Gibart, P.; Verie, C.; Bernard, C.; Schouler, M. C. *J. Cryst. Growth* **1980**, *48*, 367.

(9) Bougnot, G. J.; Foucaran, A. F.; Marjan, M.; Etienne, D.; Bougnot, J.; Delannoy, F. M. H.; Roumanille, F. M. *J. Cryst. Growth* **1986**, *77*, 400.

(10) Biefeld, R. M.; Hebner, G. A. *Appl. Phys. Lett.* **1990**, *57*, 1563.

(11) Chen, C. H.; Huang, K. T.; Drobeck, D. L.; Stringfellow, G. B. *J. Cryst. Growth* **1992**, *124*, 142.

(12) Chen, C. H.; Fang, Z. M.; Stringfellow, G. B.; Gedridge, R. W. *J. Appl. Phys.* **1991**, *69*, 7605.

(13) Baucom, K. C.; Biefeld, R. M. *Appl. Phys. Lett.* **1994**, *64*, 3021.

(14) Li, S. H.; Larsen, C. A.; Stringfellow, G. B.; Gedridge, R. W. *J. Electron. Mater.* **1991**, *20*, 457.

(15) Larsen, C. A.; Li, S. H.; Stringfellow, G. B. *Chem. Mater.* **1991**, *3*, 39.

(16) Hill, C. W.; Tao, M.; Gedridge, R. W.; Stringfellow, G. B. *J. Electron. Mater.* **1994**, *23*, 447.

(17) Berrigan, R. A.; Metson, J. B.; Russell, D. K. *Chem. Vap. Deposition* **1998**, *4*, 23.

(18) Skulan, A. J.; Nielsen, I. B.; Allendorf, M. D.; Melius, C. F. *J. Phys. Chem. A* **2006**, *110*, 281.

(19) Allendorf, M. D.; Melius, C. F. *J. Phys. Chem. A* **2005**, *109*, 4939.

(20) Wagman, D. D.; Evans, W. H.; Parker, V. B.; Schumm, R. H.; Halow, I.; Bailey, S. M.; Churney, K. L.; Nuttall, R. L. *J. Phys. Chem. Ref. Data* **1982**, *11* (Suppl. 2).

(21) Cox, J. D.; Pilcher, G. *Thermochemistry of Organic and Organometallic Compounds*; Academic Press: London, 1970.

(22) Long, L. H.; Sackman, J. F. *Trans. Faraday Soc.* **1955**, *51*, 1062.

(23) Stone, F. G. A.; West, R. *Advances in Organometallic Chemistry*; Academic Press: New York, 1964; Vol. 2.

(24) Gmelin, L. *Gmelin Handbook of Inorganic and Organometallic Chemistry. System Number 46. Sn−Organotin Compounds*; Springer: Berlin, 1975; Vol. 1.

(25) Berry, R.; Ehlers, C.; Burgess, D.; Zachariah, M.; Nyden, M.; Schwartz, M. *THEOCHEM (J. Mol. Struct.)* **1998**, *422*, 89.

(26) Allendorf, M. D.; Melius, C. F. *J. Phys. Chem. A* **1997**, *101*, 2670.

(27) Allendorf, M. D.; Melius, C. F. *J. Phys. Chem. A* **2002**, *106*, 6370.

(28) Glaude, P. A.; Curran, H. J.; Pitz, W. J.; Westbrook, C. K.; Gann, R. G. Kinetic study of the combustion of organophosphorus compounds. In *Proceedings Twenty-Eighth Symposium (International) on Combustion*; The Combustion Institute: Pittsburgh, PA, 2000; p 1749.

(29) Reaction Design, San Diego, CA.

(30) Thermochemistry DB for High-Temp Materials Synthesis; available at www.ca.sandia.gov/HiTempThermo/index.html.

(31) Peterson, K. A. *J. Chem. Phys.* **2003**, *119*, 11099.

(32) Dunning, T. H., Jr. *J. Chem. Phys.* **1989**, *90*, 1007.

(33) Metz, B.; Stoll, H.; Dolg, M. *J. Chem. Phys.* **2000**, *113*, 2563.

(34) Chase, M. W.; Davies, C. A.; Downey, J. R.; Frurip, D. J.; McDonald, R. A.; Szverud, A. N. *J. Phys. Chem. Ref. Data* **1985**, 14.

(35) Ruscic, B.; Berkowitz, J. *J. Chem. Phys.* **1993**, *99*, 5840.

(36) Chase, M. W. *NIST-JANAF Thermochemical Tables*, 4th ed.; American Institute of Physics: Washington, DC, 1998.

(37) Hehre, W. J.; Ditchfield, R.; Pople, J. A. *J. Chem. Phys.* **1972**, *56*, 2257.

(38) Frisch, M. J.; Pople, J. A.; Binkley, J. S. *J. Chem. Phys.* **1984**, *80*, 3265.

(39) Rassolov, V. A.; Ratner, M. A.; Pople, J. A.; Redfern, P. C.; Curtiss, L. A. *J. Comput. Chem.* **2001**, *22*, 976.

(40) Gugelchuk, M. M. *THEOCHEM* **1995**, *357*, 263.

(41) Niu, S. Q.; Hall, M. B. *J. Phys. Chem. A* **1997**, *101*, 1360.

(42) Szabo, A.; Ostlund, N. S. *Modern Quantum Chemistry*; Dover: New York, 1989.

(43) Hehre, W. J.; Radom, L.; Schleyer, P. v. R.; Pople, J. A. *Ab Initio Molecular Orbital Theory*; Wiley: New York, 1986.

(44) Pople, J. A.; Head-Gordon, M.; Fox, D. J.; Raghavachari, K.; Curtiss, L. A. *J. Chem. Phys.* **1989**, *90*, 5622.

(45) LaJohn, L. A.; Christiansen, P. A.; Ross, R. B.; Atashroo, T.; Ermler, W. C. *J. Chem. Phys.* **1987**, *87*, 2812.

(46) Basis sets were obtained from the Extensible Computational Chemistry Environment Basis Set Database, version 12/03/03, as developed and distributed by the Molecular Science Computing Facility, Environmental and Molecular Sciences Laboratory, which is part of the Pacific Northwest Laboratory, P.O. Box 999, Richland, WA 99352, and funded by the U.S. Department of Energy. The Pacific Northwest Laboratory is a multiprogram laboratory operated by Battelle Memorial Institute for the U.S. Department of Energy under Contract DE-AC06-76RLO 1830. Contact David Feller or Karen Schuchardt for further information.

(47) Frisch, M. J.; Trucks, G. W.; Schlegel, H. B.; Scuseria, G. E.; Robb, M. A.; Cheeseman, J. R.; Zakrzewski, V. G.; Montgomery, J. A., Jr.; Stratmann, R. E.; Burant, J. C.; Dapprich, S.; Millam, J. M.; Daniels, A. D.; Kudin, K. N.; Strain, M. C.; Farkas, O.; Tomasi, J.; Barone, V.; Cossi, M.; Cammi, R.; Mennucci, B.; Pomelli, C.; Adamo, C.; Clifford, S.; Ochterski, J.; Petersson, G. A.; Ayala, P. Y.; Cui, Q.; Morokuma, K.; Malick, D. K.; Rabuck, A. D.; Raghavachari, K.; Foresman, J. B.; Cioslowski, J.; Ortiz, J. V.; Stefanov, B. B.; Liu, G.; Liashenko, A.; Piskorz, P.; Komaromi, I.; Gomperts, R.; Martin, R. L.; Fox, D. J.; Keith, T.; Al-Laham, M. A.; Peng, C. Y.; Nanayakkara, A.; Gonzalez, C.; Challacombe, M.; Gill, P. M. W.; Johnson, B. G.; Chen, W.; Wong, M. W.; Andres, J. L.; Head-Gordon, M.; Replogle, E. S.; Pople, J. A. *Gaussian 98*; Gaussian, Inc.: Pittsburgh, PA, 1998.

(48) Ho, P.; Melius, C. F. *J. Phys. Chem.* **1990**, *94*, 5120.

(49) Allendorf, M. D.; Melius, C. F. *J. Phys. Chem.* **1992**, *96*, 428.

(50) Allendorf, M. D.; Melius, C. F. *J. Phys. Chem.* **1993**, *97*, 720.

(51) Allendorf, M. D.; Melius, C. F.; Ho, P.; Zachariah, M. R. *J. Phys. Chem.* **1995**, *99*, 15285.

(52) Mukherjee, A. U.S. Patent 4,959,257, 1990.

(53) Pitzer, K. S.; Gwinn, W. D. *J. Chem. Phys.* **1942**, *10*, 428.

(54) Benson, S. W. *Thermochemical Kinetics*, 2nd ed.; Wiley: New York, 1976.

(55) Gurvich, L. V.; Veyts, I. V.; Alcock, C. B. *Thermodynamic Properties of Individual Substances*; CRC Press: Boca Raton, FL, 1994; Vol. 3.

(56) Melius, C. F.; Allendorf, M. D. *J. Phys. Chem.* **2000**, *104*, 2168.

(57) The descriptor "ax" in structure names indicates that the unique ligand is found on the C_3 rotational axis of the ideal trigonal bipyramid. "eq" shows that the unique ligand is found on a perpendicular C_2 axis. e.g., *ax*-Sb(Cl)$_4$ refers to a molecule with an open coordination position on the C_3 axis. Any confusion can be clarified by referring to the molecular Cartesian coordinates found in the Supporting Information.

(58) Cramer, C. J. *Essentials of Computational Chemistry*; Wiley: Chichester, U.K., 2003.

(59) Bauschlicher, C. W., Jr. *J. Phys. Chem. A* **1999**, *103*, 6429.

(60) Allendorf, M. D.; Melius, C. F.; Bauschlicher, C. W. *J. Phys. IV* **1999**, *9*, 23.

(61) Walsh, R. *Acc. Chem. Res.* **1981**, *14*, 246.

(62) Melius, C. F. Lawrence Livermore National Laboratory, Livermore, CA. Unpublished results.

(63) Li, S. H.; Larsen, C. A.; Stringfellow, G. B. *J. Cryst. Growth* **1991**, *112*, 515.

(64) Daul, C.; Frioud, M.; Schafer, O.; Selloni, A. *Chem. Phys. Lett.* **1996**, *262*, 74.

(65) Melius, C. F. Thermochemistry of Hydrocarbon Intermediates in Combustion: Application of the BAC-MP4 Methodology. In *Chemistry and Physics of Energetic Materials*; Bulusu, S. N., Ed.; Kluwer Academic Publishers: Dordrecht, The Netherlands, 1990; Vol. 309, p 21.